INTERNATIONAL JOURNAL FOR NUMERICAL METHODS IN ENGINEERING, VOL. 39, 4021–4038 (1996)

ON THE REMOVAL OF RIGID BODY MOTIONS IN THE SOLUTION OF ELASTOSTATIC PROBLEMS BY DIRECT BEM

A. BLÁZQUEZ, V. MANTIČ*, F. PARÍS AND J. CAÑAS

ETSII, University of Seville, Av. Reina Mercedes s/n, 41012 Seville, Spain

SUMMARY

A theoretical and numerical study of the removal of rigid body motions in the solution of the boundary form of Somigliana identity and of the corresponding discretized linear system of the direct BEM is presented. This study is based on the Fredholm theory of linear operators and mechanical aspects of the problem. Various methods suitable for implementation in BEM codes are analyzed and relations between apparently different methods are shown. The relation between global equilibrium conditions and solvability of the discretized linear system of the direct BEM is discussed.

KEY WORDS: boundary element method; rigid-body motions; support conditions; elasticity; Fredholm theory

1. INTRODUCTION

If a two- or three-dimensional (2-D or 3-D) finite elastic body is completely free, i.e. all prescribed boundary conditions are given in stresses, or if it is improperly supported, i.e. it can freely translate and/or rotate in some directions (finitely or infinitesimally), the solution in displacements is then not unique. There are infinite solutions which generate the same stress state, the only difference between two such solutions being a rigid-body motion.

The analogy in the Theory of Potential—solution of Poisson equation—is the Neumann problem, whose solutions differ from each other by a constant.

This uncertainty in displacement solutions of some elastic Boundary Value Problems (BVP) implies singularity of the system of linear algebraic equations resulting from the discretizations of this problem. Zero eigenvalue solutions of this linear system naturally correspond to the rigid-body motions which are allowed by the given boundary conditions.

In the mathematical bibliography this difficulty in the solution of Boundary Integral Equations (BIE) is related to the Fredholm alternative.[1–3] Starting from the Fredholm theory of linear operators, two different approaches have been proposed by various authors to solve this difficulty: the first, augmenting the original non-invertible linear operator;[1,4–6] the second, adding an integral operator with a degenerate kernel to the original linear operator.[7,8]

Although various related numerical tests in solutions by indirect BEM in Elasticity[1,7,9] and Potential Theory,[5] and also some results for direct BEM can be found in Reference 10 for Elasticity

* On leave from Department of Technical Mechanics and Elasticity, Faculty of Mechanical Engineering, Technical University, Košice 04187, Slovakia

CCC 0029–5981/96/234021–18

Received 4 April 1995
Revised 3 January 1996

and in Reference 11 for Potential Theory, it seems that there is a need for a deeper numerical study and comparison of various approaches in direct BEM.

Additionally, it appears that there is a lack of a simple interpretation from an engineering point of view of some mathematically motivated methods, and a lack of emphasis on a direct relation between the Fredholm theory, rigid-body motions and global equilibrium conditions which must satisfy prescribed loads in improperly supported bodies.

The article presents various approaches suitable for implementation in BEM codes, shows relations between these at first sight different methods and gives a simple analysis of what occurs with the solutions by these methods if the global equilibrium conditions are slightly perturbed due to inaccuracies in discretizations of geometry or loads. All the approaches presented have been implemented in a 2-D BEM code and a comparative study has been performed with the aim of recommending some of them for practical computations by BEM.

2. BEM, RIGID-BODY MOTIONS AND GLOBAL EQUILIBRIUM CONDITIONS

Let us consider an elastic finite body $\mathscr{D} \subset \mathbb{R}^d$ $(d = 2,3)$ with a boundary $\partial\mathscr{D}$. For the sake of brevity, body forces will not be considered in what follows. Somigliana identity [12–14, 10] written for a boundary point x has the form of a BIE for the displacement and stress vectors, u_j and t_j, at boundary points:

$$C_{ij}(x)u_j(x) + \int\!\!\!\!\!\!-_{\partial\mathscr{D}} T_{ij}^{\psi}(x,y)u_j(y)\,\mathrm{d}s(y) = \int_{\partial\mathscr{D}} \Psi_{ij}(x,y)t_j(y)\,\mathrm{d}s(y) \quad x \in \partial\mathscr{D}, \quad i,j = 1,\ldots,d \tag{1}$$

where Ψ_{ij} is the fundamental solution of Navier equation in displacements, T_{ij}^{ψ} are the corresponding fundamental stresses and $C_{ij}(x)$ is the characteristic matrix of the free term, which depends on the local geometry of the boundary at the point x, $C_{ij}(x)$ being $\frac{1}{2}\delta_{ij}$ for 'smooth' boundary points.

A BVP with all boundary conditions given in stresses does not have a unique displacement solution, because rigid-body motions give zero stresses. In other words, if $u_i^{(1)}(x)$ and $u_i^{(2)}(x)$ are solutions of BIE (1) then $u_i^{(2)}(x) - u_i^{(1)}(x) = \mu_i(x)$, where $\mu_i(x)$ represents a rigid-body motion.

A basis of the linear space of rigid-body motions will be denoted by $\mu_i^{\alpha}(x)$ for $x \in \mathscr{D} \cup \partial\mathscr{D}$ and $\alpha = 1,\ldots,n_d$ with $n_d = 3(d-1)$. A simple example follows in 2-D:

$$\boldsymbol{\mu}^1(x) = \begin{Bmatrix} 1 \\ 0 \end{Bmatrix}, \quad \boldsymbol{\mu}^2(x) = \begin{Bmatrix} 0 \\ 1 \end{Bmatrix}, \quad \boldsymbol{\mu}^3(x) = \begin{Bmatrix} -x_2 \\ x_1 \end{Bmatrix} \tag{2}$$

By substituting the above rigid-body motions as the solution of the auxiliary problem into the second Betti theorem of reciprocity of work,[1, 14] the global equilibrium equations, due to the fact that rigid-body motions give zero stresses, are directly obtained:

$$\int_{\partial\mathscr{D}} t_i(x)\mu_i^{\alpha}(x)\,\mathrm{d}s(x) = 0 \tag{3}$$

Application of BEM to Elasticity consists of the numerical solution of BIE (1). Discretization of the boundary $\partial\mathscr{D}$ by boundary elements assuming certain evolutions of the variables of this equation along each element leads to a system of linear equations that can be represented schematically by

$$\mathbf{Hu} = \mathbf{Gt}\,(= \mathbf{b}) \tag{4}$$

Entries of the matrix $\mathbf{H} \in \mathbb{R}^{d.n \times d.n}$, with n equal to the number of nodes used in the discretization, represent integrals of stresses of fundamental solution, T_{ij}^{ψ}, times the shape functions over the boundary elements plus the free term matrix C_{ij}. Analogously, entries of the matrix $\mathbf{G} \in \mathbb{R}^{d.n \times d.n}$

represent integrals of the fundamental solution Ψ_{ij}. Vectors $\mathbf{u} \in \mathbb{R}^{d.n}$ and $\mathbf{t} \in \mathbb{R}^{d.n}$ contain displacements and boundary stress vectors at the boundary element nodes. Although without implications in the problem under consideration, it should be noted that the matrix $\mathbf{G}$ can have a greater number of columns depending on the continuity assigned to the stress vector passing from one element to an adjacent one.

Because rigid-body motions give zero stresses, $\mathbf{H}$ is a singular matrix and its null space is composed of vectors that correspond to rigid-body motions, i.e. $\text{rank}(\mathbf{H}) = d.n - n_d$. In the discretized version of BIE (4) column vectors $\mathbf{m}^\alpha$ of the following matrix $\mathbf{M} \in \mathbb{R}^{d.n \times n_d}$ form the basis of rigid-body motions used here in 2-D:

$$\mathbf{M} = [\mathbf{m}^1, \mathbf{m}^2, \mathbf{m}^3] = \begin{bmatrix} 1 & 0 & -x_2(1) \\ 0 & 1 & x_1(1) \\ \vdots & \vdots & \vdots \\ 1 & 0 & -x_2(n) \\ 0 & 1 & x_1(n) \end{bmatrix} \tag{5}$$

$\mathbf{H}$ and $\mathbf{M}$ obviously being related by

$$\mathbf{HM} = \mathbf{0} \tag{6}$$

Isoparametric straight and curved boundary elements exactly represent constant and linear functions of the spatial variables x_i.[13, 15] Thus, the accuracy of equation (6) is defined only by the accuracy of the evaluations of the integrals which form the entries of the matrix $\mathbf{H}$. On the other hand, this equation is valid only approximately for constant elements or even for curved elements with linear interpolation of the variables, which cannot represent exactly a rotation of the body.[13]

The problems presented in this study have been solved by a 2-D BEM program which uses: linear elements with the nodes at the extremes of the element but allowing discontinuities in the stress vector, collocation at nodes, analytical evaluation of singular integrals and the free term matrix, numerical integration of regular integrals by Gaussian quadratures usually with 8 points, double precision for floating point numbers (Real*8) and Gaussian elimination for solution of the linear system of equations.

3. METHODS BASED ON SIMPLE APPLICATION OF SUPPORT CONDITIONS

If the problem under consideration is analysed by BEM, linear system (4) with a theoretically singular matrix has to be solved. With increasing accuracy of quadratures used for evaluation of the matrix coefficients, the matrix will be more singular (i.e. the condition number of the matrix will increase[16]), and consequently results obtained by a direct solution of this system will be increasingly affected by roundoff errors. This fact rules out the possibility of directly solving the system (4) without modifying it in some way. These general statements are corroborated numerically in Appendix I with reference to the problems considered in this paper, which will be presented later on in this section. Therefore, methods replacing the original ill-conditioned system (4) with a well-conditioned and in a certain sense equivalent one are useful.

The usual way in engineering practice of solving this kind of BVP, with some displacements and/or rotations allowed, is the removal of the rigid-body motions from numerical solutions by placing a sufficient number of additional point supports. These supports, naturally placed at the nodes, must not introduce stresses into the problem and must inhibit all rigid body motions.

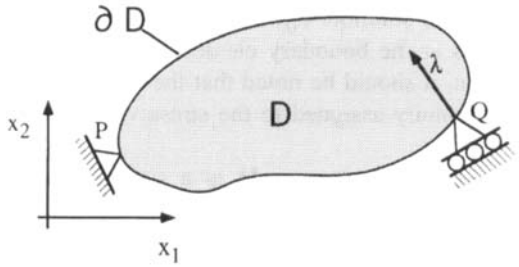

Figure 1. Example of supports that do not introduce stresses and inhibit all rigid-body motions

Figure 1 represents a 2-D problem where it is assumed that all boundary conditions are given in stresses, three-point constraints being needed to inhibit all rigid-body motions. The support conditions of Figure 1 can be written as

$$\begin{aligned} u_1(P) &= 0 \\ u_2(P) &= 0 \\ \lambda_1 u_1(Q) + \lambda_2 u_2(Q) &= 0 \end{aligned} \tag{7}$$

Simple implementation of this procedure in BEM can be achieved by replacing some collocation equations with point support conditions. It should be stressed that it is not known *a priori* which collocation equations are suitable for dropping out. Therefore, the following two methods have been examined.

First, a simple approach applying the idea successfully used in FEM[15, 17] and recommended[18] for applications in general situations, i.e. directly forcing the displacement field in the resulting linear system to satisfy additional point support conditions by putting zeros in the corresponding rows and columns of the linear system and defining the diagonal entries equal to 1 (Method S1), is applied. Second, point support equations are added to the initial system. The system then has more equations than unknowns and a procedure of column pivoting, which selects as pivot the largest entry in the column, is used to solve the resulting system by elimination of some collocation equations which are linear combinations of the others (Method S2).

All the results shown in this paper correspond to the problems shown in Figures 2(a) and 2(b), which in what follows will be denoted by 'plate' and 'ground' respectively. The analytical solutions[19] used for comparison with numerical solutions fulfill the shown point support conditions. Loads are defined by the parameter $p = 1000\,\mathrm{kg/cm^2}$ and material by Young's modulus $E = 10^6\,\mathrm{kg/cm^2}$ and Poisson's ratio $\nu = 0{\cdot}25$. Some comments are required to justify the selection of these two problems. The errors in the solution by BEM can come from the errors in discretizing the boundary (the original boundary could not coincide with the discretized boundary) and from the errors in discretizing the variables along the boundary. In the two problems selected the original boundary and the discretized boundary coincide, the only source of errors being the second cause. In the first problem the procedure of approximation of the load does not alter it (linear elements can represent exactly the piecewise linear stress vector field) and, in turn, in the second problem the approximation will alter the load. Consequently, the discretized boundary stress vector field will be globally in equilibrium in the first problem but not in the second.

Figure 3 represents the solutions of the problem of Figure 2(a) using Methods S1 and S2. Comparing these results, and although neither of them can be considered completely satisfactory because of the peaks that appear in the displacement u_2, it might seem that Method S2 leads to a better result than S1. However, it can be observed that the result using S1 is similar to

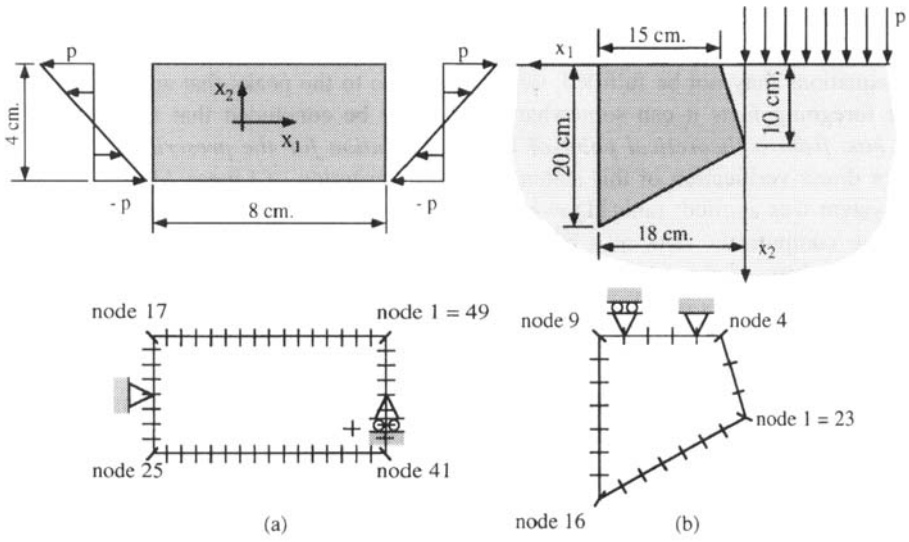

Figure 2. Geometry, boundary conditions, discretization and point supports in the analysed problems: (a) plate subjected to bending; (b) ground subjected to a semiinfinite pressure

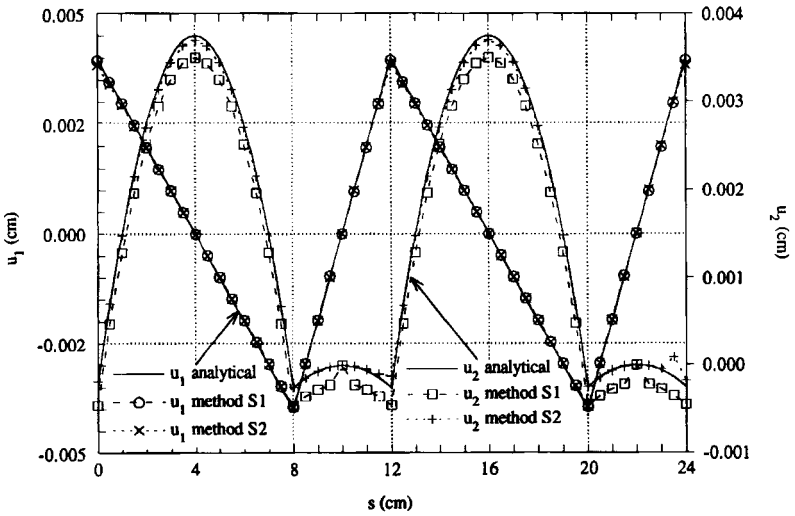

Figure 3. Plate: results of methods S1 and S2

the result using S2 if the result of S1 is appropriately translated along the axis x_2 (vertically in Figure 3). This translation is required because the peaks in the results of S1 always appear at point supports (the corresponding collocation equations have been dropped out), whereas in S2 they appear associated to the nodes (not supports in this case) and directions whose corresponding integral equations have been dropped out by the pivoting procedure.

Studying the dropped equations, the relative residuals in the original system, defined by $(H_{ij}u_j - b_i)/\|\mathbf{b}\|$, were calculated for all the equations, applying the solutions given by each method. It was observed that for at least two of the equations dropped out from the original system the residuals

were of an order 10^{-2} even if Gaussian quadrature with 16 points was used, while for the rest of the equations they were of an order $10^{-17}-10^{-18}$ or smaller. Thus, in general, dropped out collocation equations may not be fulfilled, which gives rise to the peaks that appear in the solution.

From the foregoing facts it can somewhat surprisingly be concluded that *the singular original system* (4) *has, from a theoretical point of view, no solution for the prescribed load* in the case analysed. For direct verification of this statement a basic criterion of Linear Algebra for solvability of a linear system was applied: rank($\mathbf{H}$) = rank([$\mathbf{H}$, $\mathbf{Gt}$]). According to Referece 16, the only fully reliable way to compute the rank of a matrix is Singular Value Decomposition (SVD). The four lowest singular values of the matrix $\mathbf{H}$ in decreasing order given by an SVD procedure were: $7{\cdot}5\times10^{-2}$, $2{\cdot}2\times10^{-15}$, $2{\cdot}1\times10^{-15}$, $1{\cdot}7\times10^{-15}$, and similarly for the matrix: [$\mathbf{H}$, $\mathbf{Gt}$] $7{\cdot}5\times10^{-2}$, $2{\cdot}0\times10^{-5}$, $2{\cdot}1\times10^{-15}$, $1{\cdot}7\times10^{-15}$, if the matrices were generated by 16-point Gaussian formula. This result implies rank($\mathbf{H}$) < rank([$\mathbf{H}$, $\mathbf{Gt}$]).

With reference to the problem of Figure 2(b), the displacement solution is considerably affected by the dropping out of equations. The solution obtained by Methods S1 and S2 can be considered poor, except when a very high number of elements (about 200) was used, peaks again appearing at the nodes whose equations are not fulfilled.

A general conclusion can be deduced from the numerical study presented. The initial linear system (4) may not have any displacement solution $\mathbf{u}$ for some globally equilibrated discretized loads $\mathbf{t}$, which implies that if some collocation equations are dropped out of this system there is no guarantee that a solution of the resulting system satisfactory fulfills these dropped out equations. Additionally, a strong relation between a nodal variable and the corresponding collocation equation applied at the node has been observed. Consequently, it would be desirable to propose a modification of the initial system which implies a 'suitable average' fulfillment of all the collocation equations, none of them being dropped out of the resulting system. This will be the object of the following sections.

4. METHODS BASED ON THE FREDHOLM THEORY

First, we will introduce a simple theoretical analysis of some important relations between rigid-body motions, global equilibrium conditions and boundary integral operators on the left- and right-hand side of the BIE (1). Then two methods based on this analysis, which augment or modify the original BIE and its discretized form in such a way that they become uniquely solvable, will be presented.

4.1. Removal of rigid-body motions in the original BIE

Consider for a moment that all space $\mathbb{R}^d$ is occupied by the original finite elastic body $\mathscr{D}$ and its complementary infinite body $\mathscr{D}^c$. It is assumed that $\mathscr{D}$ is a simply connected body with a smooth boundary $\partial\mathscr{D}$.

For a rigid-body motion $\mu_i^\alpha(x)$, it follows directly from BIE (1) that:

$$\frac{1}{2}\mu_i^\alpha(x) + \int\!\!\!\!\!\!-_{\partial\mathscr{D}} T_{ij}^{\psi}(x,y)\mu_j^\alpha(y)\,\mathrm{d}s(y) = 0, \quad x \in \partial\mathscr{D}, \quad \alpha = 1,\ldots,n_d \tag{8}$$

Thus, rigid-body motions are zero eigenfunctions of the second kind of boundary integral operator on the left-hand side of the BIE denoted here by $\frac{1}{2} + \mathbf{T}$.

If the behaviour of the displacement field $u_i(x)$ at infinity in the complementary body $\mathscr{D}^c$ can be described by:

$$u_i(x) = \Psi_{ij}(x,0)b_j + O(\|x\|^{1-d}), \quad x \in \mathscr{D}^c, \quad \|x\| \to \infty \tag{9}$$

where, as follows from Saint-Venant principle, the constant vector b_j must be equal to the resultant force of stresses on $\partial\mathscr{D}$:

$$b_j = \int_{\partial\mathscr{D}} t_j(y)\,\mathrm{d}s(y) \tag{10}$$

then the same form of BIE (1) is valid for $\mathscr{D}^c$ as well.[12, 13] Notation $T_{ij}^{\psi c}(x, y)$ will be adopted for the integral kernel which depends on the outward normal with respect to $\mathscr{D}^c$, $n_i^c(y) = -n_i(y)$.

Let the boundary stress vector solution of the BVPs in $\mathscr{D}^c$ with displacement boundary condition $\mu_i^\alpha(x)$ and with behaviour of the displacements at infinity defined by (9) be denoted by $\tau_i^\alpha(x)$ for $x \in \partial\mathscr{D}$ and $\alpha = 1,\ldots,n_d$. These BVPs always have unique solutions apart from the critical 2-D contours analogous to the concept of γ-contours in Potential Theory.[14] Some details and numerical tests in Elasticity can be found in Reference 20. BIE (1) in $\mathscr{D}^c$ for these BVPs takes the form

$$\begin{aligned}\int_{\partial\mathscr{D}} \Psi_{ij}(x, y)\tau_j^\alpha(y)\,\mathrm{d}s(y) &= \frac{1}{2}\mu_i^\alpha(x) + \int\!\!\!\!\!\!-_{\partial\mathscr{D}} T_{ij}^{\psi c}(x, y)\mu_j^\alpha(y)\,\mathrm{d}s(y)\\ &= \mu_i^\alpha(x), \quad x \in \partial\mathscr{D}, \quad \alpha = 1,\ldots,n_d\end{aligned} \tag{11}$$

where relation $T_{ij}^{\psi c}(x, y) = -T_{ij}^{\psi}(x, y)$ and equation (8) were used in obtaining the second equation. We refer to Heise[7] for a detailed discussion on the functions $\tau_i^\alpha(x)$ and $\mu_i^\alpha(x)$ from the point of view of the BIEs used in the indirect version of BEM. We must be aware of the usually complicated behaviour of $\tau_i^\alpha(x)$, e.g. they can contain singularities at reentrant corners of the body $\mathscr{D}^c$. In general, we do not know these functions *a priori*.

Now let us return to the original problem for the body $\mathscr{D}$. It can be shown that solutions $\tau_j^\alpha(x)$ of equations (11) are orthogonal to the image of the integral operator $\frac{1}{2} + \mathbf{T}$ and will be very useful in the description and analysis of the methods to be presented in this section.

Multiplying BIE (1) for the case of a smooth boundary by $\tau_i^\alpha(x)$ and integrating over $\partial\mathscr{D}$ gives

$$\begin{aligned}\int_{\partial\mathscr{D}} \tau_i^\alpha(x)\left\{\frac{1}{2}u_i(x) + \int\!\!\!\!\!\!-_{\partial\mathscr{D}} T_{ij}^{\psi}(x, y)u_j(y)\,\mathrm{d}s(y)\right\}\mathrm{d}s(x)&\\ = \int_{\partial\mathscr{D}} \tau_i^\alpha(x)\left\{\int_{\partial\mathscr{D}} \Psi_{ij}(x, y)t_j(y)\,\mathrm{d}s(y)\right\}\mathrm{d}s(x)&\\ = \int_{\partial\mathscr{D}} \mu_j^\alpha(y)t_j(y)\mathrm{d}s(y)&\\ = 0&\end{aligned} \tag{12}$$

where the symmetry of the Kelvin fundamental solution $\Psi_{ij}(x, y) = \Psi_{ji}(y, x)$ and equation (11) were taken into account in derivation of the second equation and global equilibrium conditions (3) in derivation of the third equation.

A classical result of Mikhlin (Reference 21, Section 45) states that the number of linearly independent vector functions orthogonal to the image of the operator $\frac{1}{2} + \mathbf{T}$ equals the number of its linearly independent zero eigenfunctions and that both are equal to n_d. Consequently, the Fredholm theory, originally developed for boundary integral operators with bounded or weakly-singular kernels, is applicable to this operator with strongly-singular integral kernel as well. Hence, $\mu_i^\alpha(x)$ form a basis of the null space of this operator and $\tau_i^\alpha(x)$ a basis of the complementary subspace orthogonal to the image of this operator.

The following important relation between the rigid-body motions $\mu_i^\alpha(x)$ and the related stress vectors $\tau_i^\alpha(x)$ is shown in Appendix II (cf. Reference 8 for the 3-D case):

$$\det\left[\int_{\partial\mathscr{D}} \mu_i^\alpha(x)\tau_i^\beta(x)\mathrm{d}s(x)\right]_{1\leqslant\alpha,\beta\leqslant n_d} \neq 0 \tag{13}$$

We can now describe two closely related methods to obtain invertible operators which will be in some reasonable sense equivalent to the original operator $\frac{1}{2}+\mathbf{T}$. We proceed either by augmenting the original BIE (1), *Method F1*:

$$\frac{1}{2}u_i^{(1)}(x)+\int_{\partial\mathscr{D}} T_{ij}^{\psi}(x,y)u_j^{(1)}(y)\,\mathrm{d}s(y)+\sum_{\alpha=1}^{n_d} w_i^\alpha(x)\omega^\alpha=\int_{\partial\mathscr{D}}\Psi_{ij}(x,y)t_j(y)\,\mathrm{d}s(y),\quad x\in\partial\mathscr{D} \tag{14a}$$

$$\int_{\partial\mathscr{D}} v_j^\alpha(y)u_j^{(1)}(y)\,\mathrm{d}s(y)=0,\quad \alpha=1,\ldots,n_d \tag{14a}$$

with both displacements $u_i^{(1)}(x)$ and real constants ω^α as unknowns, or by modifying the original BIE (1) by adding an integral operator with a degenerated kernel, *Method F2*:

$$\frac{1}{2}u_i^{(2)}(x)+\int_{\partial\mathscr{D}} T_{ij}^{\psi}(x,y)u_j^{(2)}(y)\,\mathrm{d}s(y)+\sum_{\alpha=1}^{n_d}\int_{\partial\mathscr{D}} w_i^\alpha(x)v_j^\alpha(y)u_j^{(2)}(y)\mathrm{d}s(y)$$

$$=\int_{\partial\mathscr{D}}\Psi_{ij}(x,y)t_j(y)\mathrm{d}s(y),\quad x\in\partial\mathscr{D} \tag{15}$$

with only displacements $u_i^{(2)}(x)$ as unknowns. $v_i^\alpha(x)$ and $w_i^\alpha(x)$ can be any functions satisfying the following conditions:

$$\det\left[\int_{\partial\mathscr{D}} v_i^\alpha(x)\mu_i^\beta(x)\,\mathrm{d}s(x)\right]_{1\leqslant\alpha,\beta\leqslant n_d}\neq 0 \tag{16}$$

$$\det\left[\int_{\partial\mathscr{D}} w_i^\alpha(x)\tau_i^\beta(x)\,\mathrm{d}s(x)\right]_{1\leqslant\alpha,\beta\leqslant n_d}\neq 0 \tag{17}$$

Conditions (16) and (17) are necessary and sufficient conditions of invertibility of the operators on the left-hand sides of equations (14) and (15). Chen and Zhou (Reference 1, Theorem 4.6.4) introduced a proof of this statement for Method F1. Their proof can be applied after slight amendments for Method F2 as well. It must be emphasized that conditions (16) and (17) provide a specification for a correct choice, among all the possibilities, of $v_i^\alpha(x)$ and $w_i^\alpha(x)$, which is very useful for devising computational procedures. Hereinafter in this section it will be assumed that these conditions hold.

Subtracting equations (14a) and (15), multiplying the result by $\tau_i^\beta(x)$ and integrating over $\partial\mathscr{D}$ yields

$$0+\sum_{\alpha=1}^{n_d}\left\{\int_{\partial\mathscr{D}}\tau_i^\beta(x)w_i^\alpha(x)\,\mathrm{d}s(x)\right\}\left\{\omega^\alpha-\int_{\partial\mathscr{D}} v_j^\alpha(y)u_j^{(2)}(y)\,\mathrm{d}s(y)\right\}=0 \tag{18}$$

which with condition (17) provides a basic relation between Methods F1 and F2:

$$\int_{\partial\mathscr{D}} v_j^\alpha(y)u_j^{(2)}(y)\mathrm{d}s(y)=\omega^\alpha,\quad \alpha=1,\ldots,n_d \tag{19}$$

If the boundary stress vector $t_j(y)$, $y \in \partial\mathscr{D}$, satisfies conditions of global equilibrium (3), then multiplying (14a) by $\tau_i^\beta(x)$ and integrating over $\partial\mathscr{D}$ one obtains

$$0 + \sum_{\alpha=1}^{n_d} \left\{ \int_{\partial\mathscr{D}} \tau_i^\beta(x) w_i^\alpha(x)\, \mathrm{d}s(x) \right\} \omega^\alpha = \int_{\partial\mathscr{D}} \tau_i^\beta(x) \left\{ \int_{\partial\mathscr{D}} \Psi_{ij}(x,y) t_j(y)\, \mathrm{d}s(y) \right\} \mathrm{d}s(x)$$

$$= \int_{\partial\mathscr{D}} \mu_j^\beta(y) t_j(y)\, \mathrm{d}s(y)$$

$$= 0 \tag{20}$$

Hence, in view of (17), $\omega^\alpha = 0$ and from (19) also

$$\int_{\partial\mathscr{D}} v_j^\alpha(y) u_j^{(2)}(y)\, \mathrm{d}s(y) = 0, \quad \alpha = 1, \ldots, n_d \tag{21}$$

Therefore, solutions in displacements of (14) and (15) represent two solutions of the original BIE (1). Consequently, these solutions might differ in a rigid-body motion, but, in view of (16), they have to be equal because both satisfy the same constraint equations (14b) and (21).

As follows from the previous analysis, there are an infinite many ways to choose sets of functions $v_i^\alpha(x)$ and $w_i^\alpha(x)$. Here we describe two basic ones.

In view of relation (13) we see that the most simple choice is to define $v_i^\alpha(x) = w_i^\alpha(x) = \mu_i^\alpha(x)$.

The other possibility is to keep $w_i^\alpha(x) = \mu_i^\alpha(x)$ but replacing integral conditions (14b) (and similarly in (15)) by linear pointwise constraint conditions, which can represent point support conditions familiarly used in engineering and briefly presented in Section 3 (cf. Reference 1, Section 4.7). A simple 2-D example was shown in Figure 1, condition (16) for this example, taking the form

$$\begin{vmatrix} 1 & 0 & -x_2(P) \\ 0 & 1 & x_1(P) \\ \lambda_1 & \lambda_2 & -\lambda_1 x_2(Q) + \lambda_2 x_1(Q) \end{vmatrix} = \lambda_1(x_2(P) - x_2(Q)) - \lambda_2(x_1(P) - x_1(Q)) \neq 0 \tag{22}$$

which means that the vector $\boldsymbol{\lambda}$ and the line connecting points P and Q cannot coincide.

There is an important question from a practical application point of view. What occurs with displacement solutions in the above methods if the prescribed boundary stresses are not completely self-equilibrated as a consequence of small inaccuracies in problem modelling, i.e. in approximation of the boundary and/or the boundary stresses? It is clear that although in this case the original BIE (1) has no solution, systems of BIE (14) and (15) still provide a solution, which will be examined in what follows.

Let linearly independent stress vectors $t_j^\alpha(y)$ be the solutions of the following problems:

$$\int_{\partial\mathscr{D}} \Psi_{ij}(x,y) t_j^\alpha(y)\, \mathrm{d}s(y) = w_i^\alpha(x), \quad x \in \partial\mathscr{D}, \quad \alpha = 1, \ldots, n_d \tag{23}$$

It clearly follows from (11) that if $w_i^\alpha(x)$ is taken equal to $\mu_i^\alpha(x)$, then $t_j^\alpha(y) = \tau_j^\alpha(y)$. Equations (14a) and (15) can, respectively, be rewritten, applying relation (23), as

$$\frac{1}{2} u_i^{(1)}(x) + \int_{\partial\mathscr{D}} T_{ij}^{\psi}(x,y) u_j^{(1)}(y)\, \mathrm{d}s(y) = \int_{\partial\mathscr{D}} \Psi_{ij}(x,y) \left\{ t_j(y) - \sum_{\alpha=1}^{n_d} \omega^\alpha t_j^\alpha(y) \right\} \mathrm{d}s(y), \quad x \in \partial\mathscr{D} \tag{24}$$

and

$$\frac{1}{2}u_i^{(2)}(x) + \int_{\partial\mathscr{D}} T_{ij}^{\psi}(x,y)u_j^{(2)}(y)\,ds(y) \tag{25}$$
$$= \int_{\partial\mathscr{D}} \Psi_{ij}(x,y)\left\{t_j(y) - \sum_{\alpha=1}^{n_d} t_j^{\alpha}(y)\int_{\partial\mathscr{D}} v_k^{\alpha}(z)u_k^{(2)}(z)\,ds(z)\right\} ds(y), \quad x \in \partial\mathscr{D}$$

The expressions in brackets on the right-hand sides of (24) and (25) equal each other due to (19) and represent a modified boundary stress vector. By application of a standard procedure, i.e. multiplying (24) by $\tau_i^{\beta}(x)$, integrating over $\partial\mathscr{D}$, using the symmetry of the kernel $\Psi_{ij}(x,y)$ and equation (11), it is found that this modified boundary stress vector field satisfies global equilibrium conditions

$$0 = \int_{\partial\mathscr{D}} \mu_j^{\beta}(y)\left\{t_j(y) - \sum_{\alpha=1}^{n_d} \omega^{\alpha} t_j^{\alpha}(y)\right\} ds(y), \quad \beta = 1,\ldots,n_d \tag{26}$$

Thus, the non-equilibrated part of the prescribed load $t_j(y)$ has been undertaken in both methods by a linear combination of $t_j^{\alpha}(y)$, solutions of (23), the resultant stress vector field, being consequently highly dependent on the choice of functions $w_i^{\alpha}(x)$. The coefficients of this combination are additional unknowns ω^{α} in Method F1 and perturbations of constraint equations (21) in Method F2. Their values indicate how much the equilibrium is altered by the applied boundary stresses. Obviously, displacements $u_j^{(1)}(y)$ and $u_j^{(2)}(y)$ are solutions of the BIE (1) with the same modified right-hand side. These solutions differ from each other by a rigid-body motion which depends on the choice of functions $v_i^{\alpha}(x)$ and which is defined by the subtraction of equations (14b) and (19).

4.2. Removal of rigid-body motions in the linear system

The discretized versions of the above methods presented firstly for BIEs can be written, for the case of a body occupying a general domain, as follows for *Method F1*:

$$\begin{bmatrix} \mathbf{H} & \mathbf{W} \\ \mathbf{V}^{\mathrm{T}} & 0 \end{bmatrix} \begin{Bmatrix} \mathbf{u}^{(1)} \\ \boldsymbol{\omega} \end{Bmatrix} = \begin{Bmatrix} \mathbf{Gt} \\ \mathbf{0} \end{Bmatrix} \tag{27}$$

and for *Method F2*:

$$\left[\mathbf{H} + \mathbf{W}\mathbf{V}^{\mathrm{T}}\right]\left\{\mathbf{u}^{(2)}\right\} = \{\mathbf{Gt}\} \tag{28}$$

where $\mathbf{W}, \mathbf{V} \in \mathbb{R}^{d.n \times n_d}$ and have a clear meaning according to (14) and (15). It can easily be demonstrated that the necessary and sufficient conditions for the invertibility of linear systems (27) and (28) are

$$\det\left[\mathbf{V}^{\mathrm{T}}\mathbf{M}\right] \neq 0 \tag{29}$$

and

$$\det\left[\mathbf{W}^{\mathrm{T}}\mathbf{S}\right] \neq 0 \tag{30}$$

where the column vectors of $\mathbf{M} \in \mathbb{R}^{d.n \times n_d}$, defined in (5), and $\mathbf{S} \in \mathbb{R}^{d.n \times n_d}$ form bases of the null spaces of the matrices $\mathbf{H}$ and $\mathbf{H}^{\mathrm{T}}$, respectively.

Briefly speaking, Method F1 augments the square original matrix by n_d rows and n_d columns and Method F2 adds to the original matrix a square matrix of rank n_d.

Assuming that the matrix $\mathbf{H}$ has $d.n$ linearly independent eigenvectors, the relation

$$\det\left[\mathbf{M}^{\mathrm{T}}\mathbf{S}\right] \neq 0 \tag{31}$$

can be simply demonstrated. If this condition was not fulfilled, then such a non-trivial linear combination of the columns of **S**, combination which is orthogonal to all the columns of **M** (to the null space of **H**), would exist. But simultaneously it would be orthogonal to all the eigenvectors of **H** related to non-zero eigenvalues, which is of course impossible.

Relation (31) permits the use of the known vectors $\mathbf{m}^\alpha$ as vectors $\mathbf{w}^\alpha$ in both methods. Vectors $\mathbf{m}^\alpha$ can be used as vectors $\mathbf{v}^\alpha$ as well, but vectors related with another suitable linear condition for displacements, e.g. point supports described above, can also be used.

Subtracting system (28) from the first equation of (27) and multiplying from the left by $\mathbf{S}^T$ yields

$$\mathbf{S}^T\mathbf{H}\left(\mathbf{u}^{(1)} - \mathbf{u}^{(2)}\right) = \mathbf{0} = -\mathbf{S}^T\mathbf{W}\left(\boldsymbol{\omega} - \mathbf{V}^T\mathbf{u}^{(2)}\right) \tag{32}$$

which in view of condition (30) gives a basic relation between these systems analogous to (19):

$$\mathbf{V}^T\mathbf{u}^{(2)} = \boldsymbol{\omega} \tag{33}$$

Moreover, relation (33) implies $\mathbf{H}\left(\mathbf{u}^{(1)} - \mathbf{u}^{(2)}\right) = \mathbf{0}$ which in turn implies that $\mathbf{u}^{(1)} - \mathbf{u}^{(2)}$ is a rigid-body motion.

If the original system (4) has a solution, the following natural correspondence between this system and systems (27) and (28) can be easily shown: solutions in displacements $\mathbf{u}^{(1)}$ and $\mathbf{u}^{(2)}$ of systems (27) and (28) are the solutions of (4) as well and they are equal to each other. Subtracting the first equation of (27) from (4) and then multiplying the result by $\mathbf{S}^T$ gives

$$\begin{aligned} \mathbf{H}\left(\mathbf{u} - \mathbf{u}^{(1)}\right) &= -\mathbf{W}\boldsymbol{\omega} \\ \mathbf{0} &= -\mathbf{S}^T\mathbf{W}\boldsymbol{\omega} \end{aligned} \tag{34}$$

Hence, condition (30) yields $\boldsymbol{\omega} = \mathbf{0}$ and from (33) $\mathbf{V}^T\mathbf{u}^{(2)} = \mathbf{0}$. Therefore, $\mathbf{u}^{(1)}$ and $\mathbf{u}^{(2)}$ solve (4). Consequently, $\mathbf{u}^{(1)} - \mathbf{u}^{(2)}$ is a rigid-body motion and, in view of (29), the condition $\mathbf{V}^T\left(\mathbf{u}^{(1)} - \mathbf{u}^{(2)}\right) = \mathbf{0}$ implies $\mathbf{u}^{(1)} = \mathbf{u}^{(2)}$.

Now these two methods are applied to solve problems of Figure 2, by using two different forms for **V**, but with the same **W** matrix.

First, using $\mathbf{V} = \mathbf{W} = \mathbf{M}$, constraint equations $\mathbf{V}^T\mathbf{u} = \mathbf{0}$ imply zero 'average' translation and rotation of the displacement field. If the desired position is defined by the point supports, then an obviously calculated rigid-body motion can be added to the displacement solution in such a way that the point support conditions are fulfilled by the resultant displacements.

Second, using the matrix **V** associated to point support equations. Then, the solution obtained from Method F1 is directly the solution desired. Note that, in view of (33), a rigid-body motion has to be added to the solution from Method F2 to reach the position desired.

The results obtained by both Methods F1 and F2 coincide, once an appropriate rigid-body motion is applied. Moreover, it has been observed, as was expected, that the choice of **V** does not have any significant influence on the solution, but only defines the final position of the body, selecting a displacement field among all those possible. Therefore, only the results of Method F1 for the second option of the matrix **V** are shown in the following figures.

The excellent results, Figure 4, have been obtained, with no presence of peaks in the solution, for the problem of Figure 2(a). Note that the values of ω^α for this problem were of an order $10^{-20}, 10^{-6}$ and 10^{-21}.

With reference to the problem of Figure 2(b), the results are presented in Figure 5. It can be observed that errors are small in spite of the relatively low number of boundary elements used. Some heed can be given to the larger error found in the sharpest corner (at node number 16 in Figure 2(b)), the possible reason for this being that the stress vector distributions $t_j^\alpha(y) = \tau_j^\alpha(y)$

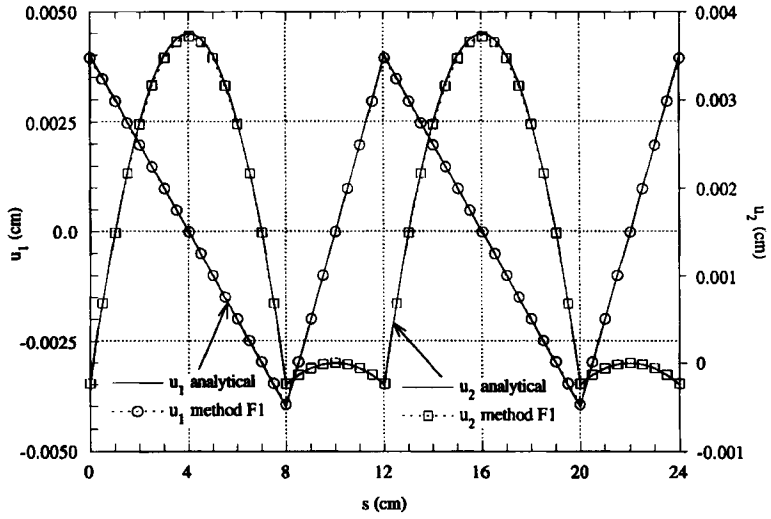

Figure 4. Plate: result of Method F1

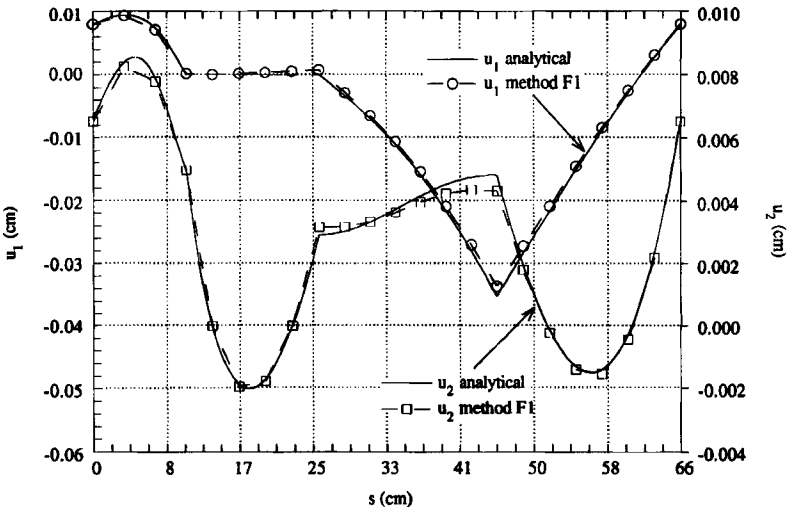

Figure 5. Ground: result of Method F1

(see (23)) used present singularities at corners of this kind. The values of ω^{α} for this problem were of an order $10^{-4}, 10^{-4}$ and 10^{-6}.

Note that Methods F1 and F2 can obviously be adapted to the cases of improperly supported bodies by using only vectors related to rigid-body motions satisfying prescribed displacement boundary conditions.

5. METHOD BASED ON CORRECTION OF STRESSES AT POINT SUPPORTS

In this section a special implementation of a physically important variant of Method F1 given by equation (27) will be presented.

Let the matrix $\mathbf{V}^{\mathrm{T}}$ be given by n_d point support equations. Without loss of generality the following partitions of the matrices $\mathbf{H} = [\mathbf{H}', \mathbf{H}'']$, $\mathbf{G} = [\mathbf{G}', \mathbf{G}'']$ and the vectors $\mathbf{u} = [\mathbf{u}', \mathbf{u}'']$, $\mathbf{t} = [\mathbf{t}', \mathbf{t}'']$ will be adopted, where the submatrices $\mathbf{H}'', \mathbf{G}'' \in \mathbb{R}^{d.n \times n_d}$ and the subvectors $\mathbf{u}'', \mathbf{t}'' \in \mathbb{R}^{n_d}$ correspond to the variables associated with point supports. Now, the matrix $\mathbf{W}$ in equation (27) is taken as $\mathbf{W} = \mathbf{G}''$, which means that its columns are generated by distributions of the stress vector over boundary elements in the neighbourhood of point supports given by the related shape functions. The first equation of (27) can be rewritten as follows:

$$\mathbf{H}\mathbf{u} = \mathbf{G}'\mathbf{t}' + \mathbf{G}''(\mathbf{t}'' - \boldsymbol{\omega}) \tag{35}$$

Therefore, constants ω^α can be interpreted as the corrections to the given nodal values of $\mathbf{t}''$ at the point supports which enable the original system (4) to have a solution. According to Section 3, constants ω^α may have relatively large values even if the values of $\mathbf{t}$ correspond to an equilibrated boundary stress vector field.

Equation (27), by applying the above adopted notation, is written:

$$\begin{bmatrix} \mathbf{H}' & \mathbf{H}'' & \mathbf{G}'' \\ \mathbf{0} & \mathbf{I} & \mathbf{0} \end{bmatrix} \begin{Bmatrix} \mathbf{u}' \\ \mathbf{u}'' \\ \boldsymbol{\omega} \end{Bmatrix} = \begin{Bmatrix} \mathbf{G}\mathbf{t} \\ \mathbf{0} \end{Bmatrix} \tag{36}$$

where $\mathbf{I}$ is the diagonal unit matrix. For implementation in BEM codes the following simplified equivalent form of this equation is suitable (*Method F1v*):

$$[\mathbf{H}', \quad \mathbf{G}''] \begin{Bmatrix} \mathbf{u}' \\ \boldsymbol{\omega} \end{Bmatrix} = \{\mathbf{G}\mathbf{t}\} \tag{37}$$

$$\mathbf{u}'' = \mathbf{0} \tag{38}$$

Qualitatively, the level of accuracy reached by this variant of Method F1 for problems of Figure 2 is, in spite of its simplicity, similar to that of the other variants of Methods F1 and F2 discussed in the previous section. Inasmuch as their results for the problem of plate almost coincide, only the result for the problem of ground is presented in Figure 6.

The values of ω^α obtained for the problem of Figure 2(a) are of an order 10^1 associated to the x_2-component in both supports, while of an order 10^{-13} when associated to the x_1-component. Therefore, the final solution of the vector of stresses, $(\mathbf{t}', \mathbf{t}'' - \boldsymbol{\omega})$, is not in global equilibrium. This result corroborates the statement that stresses in equilibrium are not necessarily a set of stresses for which the system (4) can be solved.

For the problem of Figure 2(b), whose initial discretized stresses are not in equilibrium, the values of ω^α are of orders 10^2 and 10^1 associated to the x_1- and x_2-components, respectively. It must be stated that in reducing the size of elements next to the supports, some local perturbations appear. This occurs because the area where stresses associated to ω^α are applied is smaller, so that variables ω^α have to reach higher values, thus modifying the solution locally.

Method F1v, due to the distributions $t_j^\alpha(y)$ (see (23)) used, can be considered the most straightforward way to simulate real point supports, obtaining the support forces from the values of ω^α. It should not be forgotten that these ω^α do not force equilibrium, although they generally lead to a discretized boundary load which is close to an equilibrated one.

This procedure permits the solution of problems modelled from an engineering point of view by means of point constraints and concentrated loads. These situations have been treated, as suggested in this section, by Lachat and Watson[22] and Brebbia and Dominguez,[10] among others.

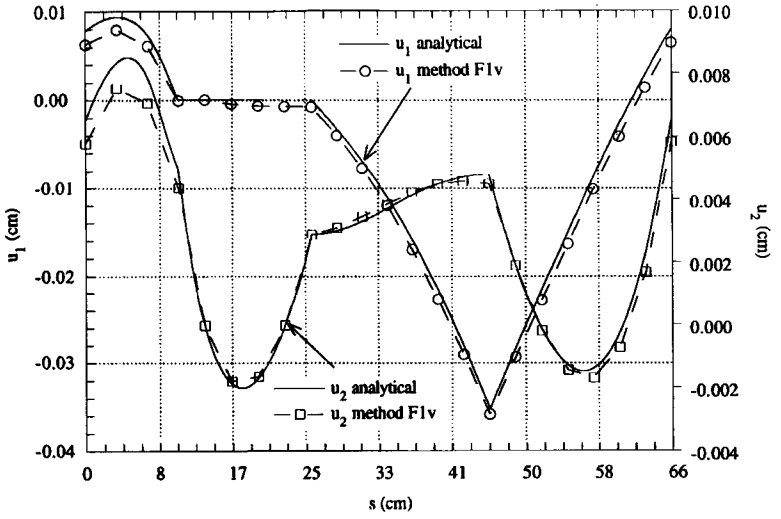

Figure 6. Ground: result of Method F1v

6. FINAL DISCUSSION AND CONCLUSIONS

The fact that the equilibrated discretized load **t** does not imply in general solvability of the linear system of equations (4) has been emphasized several times in the course of this article. It seems that the following two reasons can be given to explain why the condition of the equilibrium of this load is not exactly equivalent to the condition that the column vector **Gt** be an element of the column space of the matrix **H**. The first reason can be seen in the collocation nature of the linear system (4) and the second one in the fact that functions $\tau_i^{\alpha}(x)$, which are orthogonal to the image of the left-hand side operator of the BIE (1), generally cannot be exactly approximated by boundary element shape functions.

Accordingly, the two subspaces of the discretized boundary loads **t**, one containing loads satisfying global equilibrium and the other containing loads for which system (4) has a solution, can be different. Consequently, the question of how distant a load **t** related with a solution of (4) can be from all the globally equilibrated loads does arise. The notion of *distance between equidimensional subspaces*[16] can give an answer to this question. An important feature of this distance is that it represents the maximum relative difference between a non-zero equilibrated load vector **t** and the nearest vector to it for which equation (4) has a solution. It is naturally expected that a mesh refinement implies a decrease in this distance, but further investigation of this global error bound is considered necessary.

The relatively poor behaviour of Methods S1 and S2 has been attributed to the above discussed fact. Note that they can be interpreted as implementations of a variant of method F1 as well; e.g., Method S1 is obtained by defining $\mathbf{W} = \mathbf{V}$, where the matrix $\mathbf{V}^{\mathrm{T}}$ is given by point support equations. But in this case the matrix **W** has only a few non-zero rows, so all error in the system is concentrated in a few collocation equations (dropped out in our implementation). The consequence of this is peaks in displacement variables associated to collocation equations which are not fullfilled. Obviously, Methods S1 and S2 work if the original system (4) has a solution. This is the case of the plate subjected to pure traction analysed by linear elements or the plate subjected to bending analysed by quadratic elements.

On the other hand, if the traction Hypersingular BIE (HBIE) is discretized by the Galerkin method,[23] then functions orthogonal to the image of the left-hand side hypersingular symmetrical operator represent rigid-body displacements $\mu_i^\alpha(x)$, which are at the same time unit eigenvectors of the adjoint operator to the strongly singular operator on the right-hand side of the HBIE. Inasmuch as $\mu_i^\alpha(x)$ can be exactly represented by element shape functions, we can appreciate that the HBIE 'corresponding' to (4), discretized by the Galerkin method, will always have solutions for any equilibrated discretized loads, and both methods S1 and S2 will be able to work very well.

This is an appropriate point to reflect on the difference, in simple terms, between FEM and classical BEM, with reference to the application of the methods discussed to remove rigid-body motions. When the original system of equations corresponding to the discretized body has a solution, which is always the case for equilibrated loads in FEM, linear dependent equations can be removed, a smooth solution without peaks appearing. However, when the system has no solution, which can be the case of classical BEM with equilibrated loads, the removal of any equation implies the appearance of peaks in the solution, one approach in some way averaging the error then being required.

Theoretical analysis given in Section 4.1 helped us to give mechanical explanations to somewhat algebraically introduced numerical Methods F1 and F2 in Section 4.2. The error of a displacement solution is distributed along the boundary in accordance with chosen functions $t_j^\alpha(y)$ (see (23)). In this study only $t_j^\alpha(y) = \tau_j^\alpha(y)$ has been tested, the 'unavoidable' errors of displacement solutions obtained always being smoothly distributed along the boundary.

An interesting connection between Method F1 here proposed and numerically checked and an approach suggested by Vable[9] is developed in Appendix III.

Operator $\frac{1}{2} + \mathbf{T}$ is in general very suitable for application of iterative Krylov methods (conjugate gradients, etc.) to the solution of the resulting linear system. The convergence rates of these methods seem to be dependent on the eigenvalues of the linear system, real and clustered spectrum usually yielding rapid convergence.[5] The application of Heise's idea[7] to this operator (see Reference 11 for Potential Theory) leads to our proposal to apply these solvers to the resulting linear system of method F2 with $\mathbf{W}\mathbf{V}^{\mathrm{T}} = \frac{1}{2}\tilde{\mathbf{M}}\tilde{\mathbf{M}}^{\mathrm{T}}$. For definition of the matrix $\tilde{\mathbf{M}}$ see Appendix I.

It should be observed that the usual method applied for removing rigid-body motions in BEM codes[10, 22] has not appeared completely consistent with BEM discretization principles, which assume that stress vector is defined over boundary elements and not at nodes, and moreover that the type of boundary conditions cannot change along elements. Nevertheless, in Section 5 it was demonstrated that this classical approach can be included as a particular implementation of Method F1 at the expense of the proof of the fulfillment of condition (30).

Even though for a definite recommendation on 'how to remove rigid body motions in BEM codes' more numerical tests ought to be carried out, we can state that it should be done in a general framework of Methods F1 and F2 and that the 'decisive' factor is the choice of the matrix $\mathbf{W}$. This matrix determines the smooth distribution of 'unavoidable' errors in displacements and consequently has a considerable influence on stress solutions. From the two possibilities introduced in this work, $\mathbf{W} = \mathbf{M}$ and $\mathbf{G}''$, it seems that the first will give, in general, smoother distributions of displacement errors.

ACKNOWLEDGEMENT

The authors acknowledge the financial support given to one of them (V.M.) from the Comisión Interministerial de Ciencia y Tecnología of Spain under Grant No. SB93-A00474386.

APPENDIX I

Details of some numerical results

The objective of this appendix is to give a few numerical results that will characterize robustness and effectiveness of the methods dealt with in the previous sections. For this purpose the condition number of the linear system matrices, as a measure of their singularity, has been examined. Additionally, the influence of this condition number on the solution error is shown.

The number of points used in Gaussian quadratures is denoted by n_G. The condition number κ_2 of the linear system matrix has been computed using an SVD procedure[16] by means of formula $\kappa_2 = \sigma_{max}/\sigma_{min}$, where σ_{max} and σ_{min} are, respectively, the maximum and minimum singular values of the system matrix. The relative error, denoted by e, of relative displacements between nodes 1 and 17 for the plate subjected to bending, Figure 2(a), has been calculated by means of the formula $e = (\Delta u_1^{anal.} - \Delta u_1^{num.})/\Delta u_1^{anal.}$, where $\Delta u_1 = u_1(17) - u_1(1)$. For the direct solution of (4), a rigid-body motion has been added to the resulting displacements to fulfill the point support conditions before calculating this relative error.

With reference to Methods S1, S2, F1, F2 and F1v, point support conditions shown in Figure 2 have been applied in all of them. The matrix $\mathbf{W}$ in Methods F1 and F2 has been taken equal to $\mathbf{M}$. Variants of the Methods F1 and F2 denoted as F1* and F2* are defined by $\mathbf{V} = \mathbf{W} = \tilde{\mathbf{M}}/\sqrt{2}$, where columns of $\tilde{\mathbf{M}}$ are orthonormalized columns of the matrix $\mathbf{M}$. In fact, $\tilde{\mathbf{m}}^\alpha = \mathbf{m}^\alpha/\|\mathbf{m}^\alpha\|$, taking the centroid of the boundary nodes as the origin of the co-ordinate system (cf. Reference 7).

From Table I it can be observed that the order of the condition number κ_2 of the system *matrix* in the direct solution, matrix $\mathbf{H}$, increases considerably with increasing precision of Gaussian quadratures, which implies large roundoff errors in numerical solution of this system with a 'catastrophic effect' on errors of the relative displacements computed. In turn, κ_2 of the system matrix in Method F1 is relatively small and independent of n_G, i.e. it is independent of the condition number of the matrix $\mathbf{H}$ included in the linear system (27), which corroborates the robustness and effectiveness of this method. The error e computed by F1 does not improve with increasing n_G, the best value being achieved already for $n_G = 4$. This fact can be attributed to the regularity of the mesh, which in this case is formed by elements of equal length.

The condition numbers κ_2 of the linear system matrices of all the methods proposed in this paper are examined in Table II. Values of κ_2 have been observed to be almost independent of n_G, and therefore they are only shown for $n_G = 8$. The minimum values of κ_2 have been achieved for Methods F1* and F2* with the matrices $\mathbf{W}$ and $\mathbf{V}$ suitably defined for this purpose. All these methods provide a relatively small condition number, which corroborates their effectiveness in replacing the original ill-conditioned system with a well-conditioned one.

Table I. Plate: condition numbers and relative errors of deformations using direct solution and Method F1

	n_G	4	8	16
Direct	κ_2	$1{\cdot}08 \times 10^7$	$2{\cdot}25 \times 10^{12}$	$4{\cdot}99 \times 10^{15}$
solution	e	$-6{\cdot}32 \times 10^{-2}$	$1{\cdot}25$	$1{\cdot}94 \times 10^7$
Method F1	κ_2	424·7	424·7	424·7
	e	$-6{\cdot}72 \times 10^{-3}$	$-6{\cdot}73 \times 10^{-3}$	$-6{\cdot}73 \times 10^{-3}$

Table II. Plate and ground: condition numbers for different methods

	Method	S1	S2	F1	F2	F1v	F1*	F2*
Plate	κ_2	123	26·2	424·7	398·7	27·6	12·8	12·7
Ground	κ_2	375·1	33·2	2215	2108·7	537·5	13·9	13·8

APPENDIX II

Proof of a relation between $\boldsymbol{\mu}^\alpha$ and $\boldsymbol{\tau}^\alpha$

In this appendix relation (13) is proved. Let us assume for a moment that the relevant determinant ($n_d \times n_d$) is zero. This implies that there is a non-zero linear combination $\tilde{\tau}_j(y) = \sum_{\beta=1}^{n_d} c^\beta \tau_j^\beta(y)$ which satisfies all global equilibrium conditions (3) and generates, integrating with the kernel $\Psi_{ij}(x, y)$, a continuous displacement field $\tilde{u}_i(x)$ in $\mathbb{R}^d$:

$$\tilde{u}_i(x) = \int_{\partial\mathscr{D}} \Psi_{ij}(x, y)\tilde{\tau}_j(y)\,\mathrm{d}s(y), \quad x \in \mathbb{R}^d \tag{39}$$

which obviously satisfies Navier equation in the domains $\mathscr{D}$ and $\mathscr{D}^c$ separately and on the boundary $\partial\mathscr{D}$ equals a rigid body motion $\tilde{\mu}_i(x)$. The regularity conditions at infinity: for displacements $\tilde{u}_i(x) = O(\|x\|^{1-d})$ and for the pertinent stresses $\tilde{\sigma}_{ij}(x) = O(\|x\|^{-d})$, $x \in \mathscr{D}^c$, $\|x\| \to \infty$, follow directly from the representation (39) (cf. Reference 14). Let $\tilde{\tau}_i^{\mathscr{D}}(x)$ and $\tilde{\tau}_i^{\mathscr{D}^c}(x)$, $x \in \partial\mathscr{D}$, denote, respectively, boundary stress vectors pertinent to the displacement fields $\tilde{u}_i(x)$ defined on the domains $\mathscr{D}$ and $\mathscr{D}^c$ separately, the corresponding outward normals $n_i(x)$ and $n_i^c(x)$ being applied in the definitions of the stress vectors. From the well-known boundary jump relations for the stress vector of the simple layer potential[1, 8] it follows that $\tilde{\tau}_i(x) = \tilde{\tau}_i^{\mathscr{D}}(x) + \tilde{\tau}_i^{\mathscr{D}^c}(x)$, $x \in \partial\mathscr{D}$. Then

$$0 = \int_{\partial\mathscr{D}} \tilde{\mu}_i(x)\tilde{\tau}_i(x)\,\mathrm{d}s(x) = \int_{\partial\mathscr{D}} \tilde{\mu}_i(x)\tilde{\tau}_i^{\mathscr{D}}(x)\,\mathrm{d}s(x) + \int_{\partial\mathscr{D}} \tilde{\mu}_i(x)\tilde{\tau}_i^{\mathscr{D}^c}(x)\,\mathrm{d}s(x) \tag{40}$$

The theorem of work and energy separately applied to the displacement fields $\tilde{u}_i(x)$ in the domains $\mathscr{D}$ and $\mathscr{D}^c$ implies that the two integrals on the right-hand side of (40) represent the pertinent elastic strain energies in these domains. Therefore both energies equal zero and consequently the displacement field $\tilde{u}_i$ is a rigid-body motion in the whole space $\mathbb{R}^d$. This yields $\tilde{\tau}_i^{\mathscr{D}}(x) = \tilde{\tau}_i^{\mathscr{D}^c}(x) = 0$ and finally $\tilde{\tau}_i(x) = 0$, which concludes the proof.

APPENDIX III

A note on Vable's algorithm

The resulting displacement field $\mathbf{u}^{(V)}$ of the algorithm proposed by Vable (Reference 9, Appendix II.3) for removing rigid-body motions in direct BEM can be written, concentrating all the steps of the algorithm in one equation and applying our notation, as the solution of the following modified system:

$$(\mathbf{H} + \mathbf{W}\mathbf{V}^{\mathrm{T}})\,\mathbf{u}^{(V)} = \mathbf{G}\mathbf{t} - \mathbf{W}\left(\mathbf{V}^{\mathrm{T}}(\mathbf{H} + \mathbf{W}\mathbf{V}^{\mathrm{T}})^{-1}\mathbf{W}\right)^{-1}\mathbf{V}^{\mathrm{T}}(\mathbf{H} + \mathbf{W}\mathbf{V}^{\mathrm{T}})^{-1}\mathbf{G}\mathbf{t} \tag{41}$$

Multiplying equation (41) times $\mathbf{V}^{\mathrm{T}}(\mathbf{H} + \mathbf{W}\mathbf{V}^{\mathrm{T}})^{-1}$ from the left gives directly $\mathbf{V}^{\mathrm{T}}\mathbf{u}^{\mathrm{V}} = \mathbf{0}$. Hence, $\mathbf{u}^{(V)}$ is a solution of the original system (4) with the modified right-hand side by a linear combination of columns of $\mathbf{W}$. Inasmuch as this linear combination is uniquely defined by coefficients

ω (see Section 4.2), solution $\mathbf{u}^{(V)}$ equals solution $\mathbf{u}^{(1)}$ of (27) theoretically, i.e. omitting rounding errors of numerical computations. Moreover, application of the following interesting and easily provable identity:

$$\mathbf{V}^{\mathrm{T}}\left(\mathbf{H}+\mathbf{W}\mathbf{V}^{\mathrm{T}}\right)^{-1}\mathbf{W}=\mathbf{I} \tag{42}$$

substantially simplifies the right-hand side of (41) as follows:

$$\left(\mathbf{H}+\mathbf{W}\mathbf{V}^{\mathrm{T}}\right)\mathbf{u}^{(V)}=\mathbf{G}\mathbf{t}-\mathbf{W}\mathbf{V}^{\mathrm{T}}\left(\mathbf{H}+\mathbf{W}\mathbf{V}^{\mathrm{T}}\right)^{-1}\mathbf{G}\mathbf{t} \tag{43}$$

REFERENCES

1. G. Chen and J. Zhou, *Boundary Element Methods*, Academic Press, London, 1992.
2. R. Kress, *Linear Integral Equations*, Springer, Berlin, 1989.
3. S. Prössdorf and V.G. Maz'ya, *Linear and Boundary Integral Equations*, Springer, Berlin, 1991.
4. M. Costabel, 'Principles of boundary element methods', *Comput. Phys. Reports*, **6**, 243–274 (1987).
5. A. Greenbaum, L. Greengard and G. B. McFadden, 'Laplace's equation and the Dirichlet-Neumann map in multiply connected domains', *J. Comput. Phys.*, **105**, 267–278 (1993).
6. G. Hsiao and W. L. Wendland, 'On a boundary integral method for some exterior problems in elasticity', *Proc. Tbiliski University*, Tbiliski University Press, 1985, pp. 30–60.
7. U. Heise, 'Removal of the zero eigenvalues of integral operators in elastostatic boundary value problems', *Acta Mech.* **41**, 41–61 (1981).
8. A. G. Ugodchikov and N. M. Khutorianskii, *Boundary Element Method in the Mechanics of the Deformable Solid Body* (in Russian), Kazan University Publishers, Kazan, 1986.
9. M. Vable, 'Importance and use of rigid body mode in boundary element method', *Int. j. numer. methods eng.*, **29**, 453–472 (1990).
10. C. A. Brebbia and J. Dominguez, *Boundary Elements, An Introductory Course*, CMP, Southampton, 1992.
11. R. Vodička, 'Iterative methods for linear system solution in BEM', *Diploma Thesis*, Czech Technical University of Prague, 1993 (in Slovak).
12. J. Baláš, J. Sládek and V. Sládek, *Stress Analysis by Boundary Element Methods*, Elsevier, Amsterdam, 1989.
13. C. A. Brebbia, J. C. F. Telles and L. C. Wrobel, *Boundary Element Techniques, Theory and Applications in Engineering*, Springer, Berlin, 1984.
14. M. A. Jaswon and G. T. Symm, *Integral Equation Methods in Potential Theory and Elastostatics*, Academic Press, London, 1977.
15. B. Szabó and I. Babuška, *Finite Element Analysis*, Wiley, New York, 1991.
16. G. H. Golub and C. F. Van Loan, *Matrix Computations*, 2nd edn, Johns Hopkins, Baltimore, 1989.
17. O. C. Zienkiewicz, *The Finite Element Method*, McGraw-Hill, New York, 1977.
18. A. Jennings and J. J. McKeown, *Matrix Computation*, Wiley, Chichester, 1992.
19. S. P. Timoshenko and J. N. Goodier, *Theory of Elasticity*, 3rd edn, McGraw-Hill, New York, 1970.
20. G. Kuhn, G. Löbel and I. Potrč, Kritisches Losungverhalten der Randelementmethode mit logaritmischen Kern, *ZAMM* (1986).
21. S. G. Mikhlin, *Multidimensional Singular Integrals and Integral Equations*, Pergamon Press, Oxford, 1965.
22. J. C. Lachat and J. O. Watson, 'Progress in the use of boundary integral equations, illustrated by examples', *Comput. Methods Appl. Mech. Eng.*, **10**, 273–289 (1977).
23. S. Sirtori, G. Maier, G. Novati and S. Miccoli, 'A Galerkin symmetric boundary-element method in elasticity: formulation and implementation', *Int. j. numer. methods eng.*, **35**, 255–282 (1992).